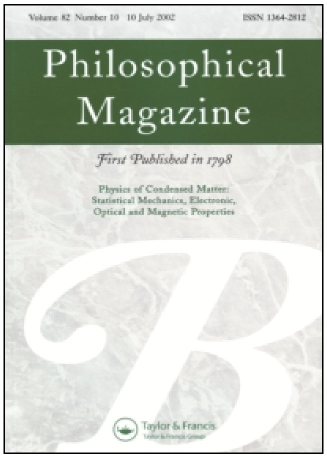

Philosophical Magazine Part B
Publication details, including instructions for authors and subscription information:
http://www.informaworld.com/smpp/title~content=t713836176

Pentagonal phases as a transient state of the reversible icosahedral-rhombohedra1 transformation in Al-Fe-Cu

N. Menguy [a]; M. Audier [a]; P. Guyot [a]; M. Vacher [a]
[a] Laboratoire de Thermodynamique et Physico-Chimie Métallurgiques, Unité associeé au CNRS 29, Ecole Nationale Supérieure d' Electrochimie et d' Electrométallurgie de Grenoble, BP, France

Online Publication Date: 01 November 1993
To cite this Article: Menguy, N., Audier, M., Guyot, P. and Vacher, M. (1993) 'Pentagonal phases as a transient state of the reversible icosahedral-rhombohedra1 transformation in Al-Fe-Cu', Philosophical Magazine Part B, 68:5, 595 - 606
To link to this article: DOI: 10.1080/13642819308220145
URL: http://dx.doi.org/10.1080/13642819308220145

PHILOSOPHICAL MAGAZINE B, 1993, VOL. 68, NO. 5, 595–606

Pentagonal phases as a transient state of the reversible icosahedral–rhombohedral transformation in Al–Fe–Cu

By N. MENGUY, M. AUDIER, P. GUYOT and M. VACHER

Laboratoire de Thermodynamique et Physico-Chimie Métallurgiques, Unité associeé au CNRS 29, Ecole Nationale Supérieure d'Electrochimie et d'Electrométallurgie de Grenoble, BP 75, 38402 St Martin d'Hères, France

[*Received 22 March 1993 and accepted 11 May 1993*]

ABSTRACT

From a transmission electron microscopy study, a transient state of the icosahedral-to-rhombohedral transformation in Al–Fe–Cu has been characterized as being constituted of an alternate mixing of two pentagonal structures. These pentagonal phases have been identified from high-resolution electron microscopy and diffraction patterns. The linear phason fields relating their structure to the icosahedral phase have been fully determined. Such a transient state results from the transformation of a modulated icosahedral phase, itself obtained from the icosahedral state and precedes the formation of the crystalline multidomain structure of the rhombohedral phase. The interpretation proposed for the formation of these pentagonal phases can be related to that given in a previous paper on the modulated icosahedral state, where the modulation was found to result from the propagation of phason waves along fivefold directions of the six-dimensional hyperspace.

§ 1. INTRODUCTION

It has been reported that for the $Al_{63\cdot5}Fe_{12\cdot5}Cu_{24}$ alloy composition the icosahedral phase is only stable at high temperatures (Bancel 1989, 1991, Audier, Guyot and Bréchet 1990). When very slowly cooled from 820°C, this quasicrystalline state undergoes a phase transition towards a crystalline multidomain structure of a rhombohedral phase ($a_R = 32{\cdot}16$ Å; $\alpha = 36°$). Domains of about 200 Å in size, are coherently oriented along each of the ten threefold axes of the icosahedron. They produce altogether an overall icosahedral symmetry, but with a characteristic splitting of the Bragg reflections (Audier and Guyot 1989, 1990). This phase transition is reversible and occurs at around 675°C through different transient states (Menguy, Audier and Guyot 1992a). Modulated icosahedral structures which transform afterwards into a mixing of two platelet structures have been observed as such intermediate states of the icosahedral-to-rhombohedral transformation. Although both the initial and the final states are chemically homogeneous, the formation of modulated icosahedral structures implies not only a lattice change but also a chemical composition variation as found from X-ray energy-dispersive spectroscopy analyses.

It has been demonstrated that the rhombohedral state is an approximant structure of the icosahedral phase and can be generated by a cut-and-projection method of the six-dimensional F-hypercubic lattice (Calvayrac *et al.* 1990), where the cut is performed along a hyperplane spanned by three fivefold vectors, for instance ($42222\bar{2}$), ($242\bar{2}22$) and ($224\bar{2}\bar{2}2$) using the indexing system of Cahn, Shechtman and Gratias (1986). More recently, Ishii (1989, 1990) has shown that the formation of the rhombohedral structure can be interpreted as resulting of phasons linearly correlated as first developed by

Lubensky *et al.* (1986) and afterwards by Qiu and Jaric (1989) and Gratias (1992), giving rise to diffuse scattering with a characteristic shape (Ishii 1992, Jaric and Nelson 1988).

A modulated icosahedral phase studied in a single-crystal X-ray diffraction experiment (Menguy *et al.* 1992b, 1993c) has been interpreted, according to this theoretical point of view, as resulting from sine waves propagating along the basis vectors of the six-dimensional (6D) hypercubic cell; in agreement with a model proposed by Janssen (1991) the polarization vectors of such waves have been found to be longitudinal, that is parallel to a fivefold axes in the perpendicular space.

Since the modulated icosahedral structure transforms into a mixing of two platelet structures before the rhombohedral state formation, it appears that the identification of these structures is required for further progress in the understanding of the transition.

We have applied the linear phason strain field theory to identify these platelet structures in order to be coherent with the analysis of the modulated icosahedral state (Menguy *et al.* 1992b, 1993c). An example of the application of such theory has been already given in a previous paper related to a characterization of the phason–phonon-assisted epitaxy at icosahedral–decagonal interfaces in Al–Pd–Mn quasicrystals (Menguy *et al.* 1993a). In § 2, we report the analysis of the experimental results from which the linear phason field expressions are determined; in § 3, we discuss which particular theoretical aspects must be considered in order to achieve a good agreement with the experimental results.

§ 2. Analysis of the experimental results

Let us recall that, from electron diffraction investigations, the formation of the two platelet structures corresponds to the appearance of new reflections near to the icosahedral reflections (Menguy *et al.* 1992a); these new reflections are periodic along fivefold icosahedral axes according to two different periodicities which are in the golden mean ratio or almost so. As observed on corresponding high-resolution electron micrographs, the platelets exhibit periodic fringes at either 10·45 or 16·9 Å parallel to their large interface planes and perpendicular to fivefold icosahedral directions. Figure 1 is an example of a high-resolution electron micrograph of this structural state viewed along a twofold zone axis of the icosahedral parent phase. The periods of 52·25 Å (= 5 × 10·45 Å) and 84·53 Å (= 5 × 16·905 Å) indicated at the edge of the micrograph will be justified later, with respect to the formalism proposed by Gratias (1992).

Linear strain field analyses have been carried out from computer Fourier transforms of high-resolution electron microscopy (HREM) images, in the same way as used for the study on local strains in an Al–Pd–Mn icosahedral matrix containing precipitates of a coherent decagonal phase (Menguy *et al.* 1993a). Computer Fourier transforms of both types of platelet are shown in figs. 2 (*a*) and (*a*′) and correspond respectively to the platelets of periods 10·45 and 16·9 Å. In figs. 2 (*b*) and (*b*′) the reflection positions observed in figs. 2 (*a*) and (*a*′) are compared with those of a perfect icosahedral state, as they have been observed before its transformation; it can be seen that the direction of the periodic reflection rows are parallel to a fivefold direction situated in the plane of these patterns. The reflections of the transformed phases have been given the indices of the closest strongest reflections of the perfect icosahedral phase pattern. This is given in the table, together with the corresponding $|\mathbf{Q}_{/\!/}|$ and $|\mathbf{Q}_{\perp}|$ and components $\Delta\mathbf{Q}_{/\!/x}$ and $\Delta\mathbf{Q}_{\perp y}$ of the spot shift $\Delta\mathbf{Q}_{/\!/}$, with respect to the perfect icosahedral phase:

$$\Delta\mathbf{Q}_{/\!/} = \mathbf{Q}_{/\!/\,\mathrm{ico}} - \mathbf{Q}_{/\!/\,\mathrm{tr\,ph}}. \tag{1}$$

Fig. 1

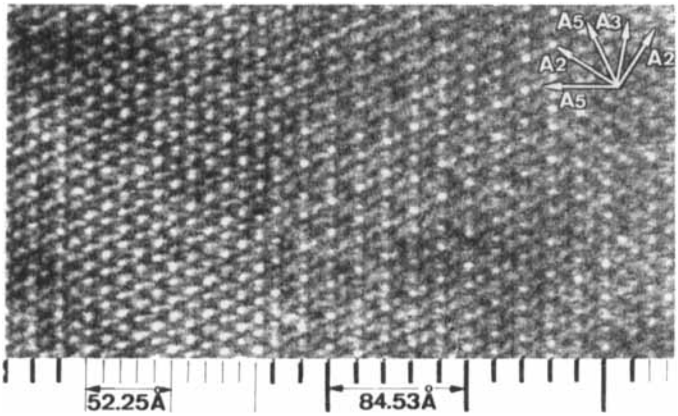

High-resolution electron micrograph showing the two types of platelet constituting a transient state of the reversible icosahedral-to-rhombohedral transformation in Al–Fe–Cu. Each type of platelet exhibits only periodic fringes at 52·25 Å/5 = 10·45 Å or 84·53 Å/5 = 16·9 Å, which remain perpendicular to a fivefold axis of the icosahedral state observed before its *in-situ* transmission electron microscopy transformation by heating. The previous orientation of the icosahedral state is indicated by axes of the icosahedral symmetry point group.

Then on the basis of theoretical models (Qiu and Jaric 1989, Lubensky *et al.* 1986, Ishii 1989, Gratias 1992), the $\Delta\mathbf{Q}_{/\!/}$ shifts may be assumed as resulting from a simple first-order linear strain field with phason ($\varepsilon_{/\!/\perp}$) and phonon ($\varepsilon_{/\!/\,/\!/}$) components:

$$\Delta\mathbf{Q}_{/\!/} = \varepsilon_{/\!/\perp}\mathbf{Q}_{\perp\mathrm{ico}} + \varepsilon_{/\!/\,/\!/}\mathbf{Q}_{/\!/\mathrm{ico}}, \tag{2}$$

where phason–phonon coupling effects are neglected; $\varepsilon_{/\!/\perp}$ and $\varepsilon_{/\!/\,/\!/}$ are respectively (2×2) matrices for phason and phonon shear fields since the HREM yields only two-dimensional images of the strain field. Both sets of values $\Delta\mathbf{Q}_{/\!/}$, as expressed in eqn. (2), are adjusted to those deduced from experiment (table) using a refinement procedure (Simon, Lyon and de Fontaine 1985). As a result of these fits, we have found the following.

(1) The matrix coefficients representing phonon fields are negligible for both the 10·45 Å and the 16·9 Å platelets.

(2) The matrix coefficients for phason fields can be expressed as a function of the golden mean τ, such that

$$\varepsilon_{/\!/\perp}10{\cdot}45 = \begin{bmatrix} -0{\cdot}06503 & -0{\cdot}03933 \\ +0{\cdot}10552 & +0{\cdot}06531 \end{bmatrix} \approx \Phi_{10\cdot45}\begin{bmatrix} -1 & -\tau^{-1} \\ \tau & 1 \end{bmatrix}, \tag{3}$$

(where $\Phi_{10\cdot45} = 0{\cdot}06531 \approx (-1/\tau^2)^2(1/5^{1/2})$) and

$$\varepsilon_{/\!/\perp}16{\cdot}9 = \begin{bmatrix} +0{\cdot}023185 & +0{\cdot}015201 \\ -0{\cdot}040939 & -0{\cdot}020403 \end{bmatrix} \approx \Phi_{16\cdot9}\begin{bmatrix} -1 & -\tau^{-1} \\ \tau & 1 \end{bmatrix} \tag{4}$$

(where $\Phi_{16\cdot9} = -0{\cdot}02492 \approx (-1/\tau^2)^3(1/5^{1/2})$).

Using these matrices now to recalculate $\Delta\mathbf{Q}_{/\!/}$, via eqns. (1) and (2), reproduces quite well the positions of the experimental reflection positions as shown in figs. 2 (*c*) and (*c*′). These (2×2) matrices (3) and (4) must be completed in three dimensions by adding one

Fig. 2

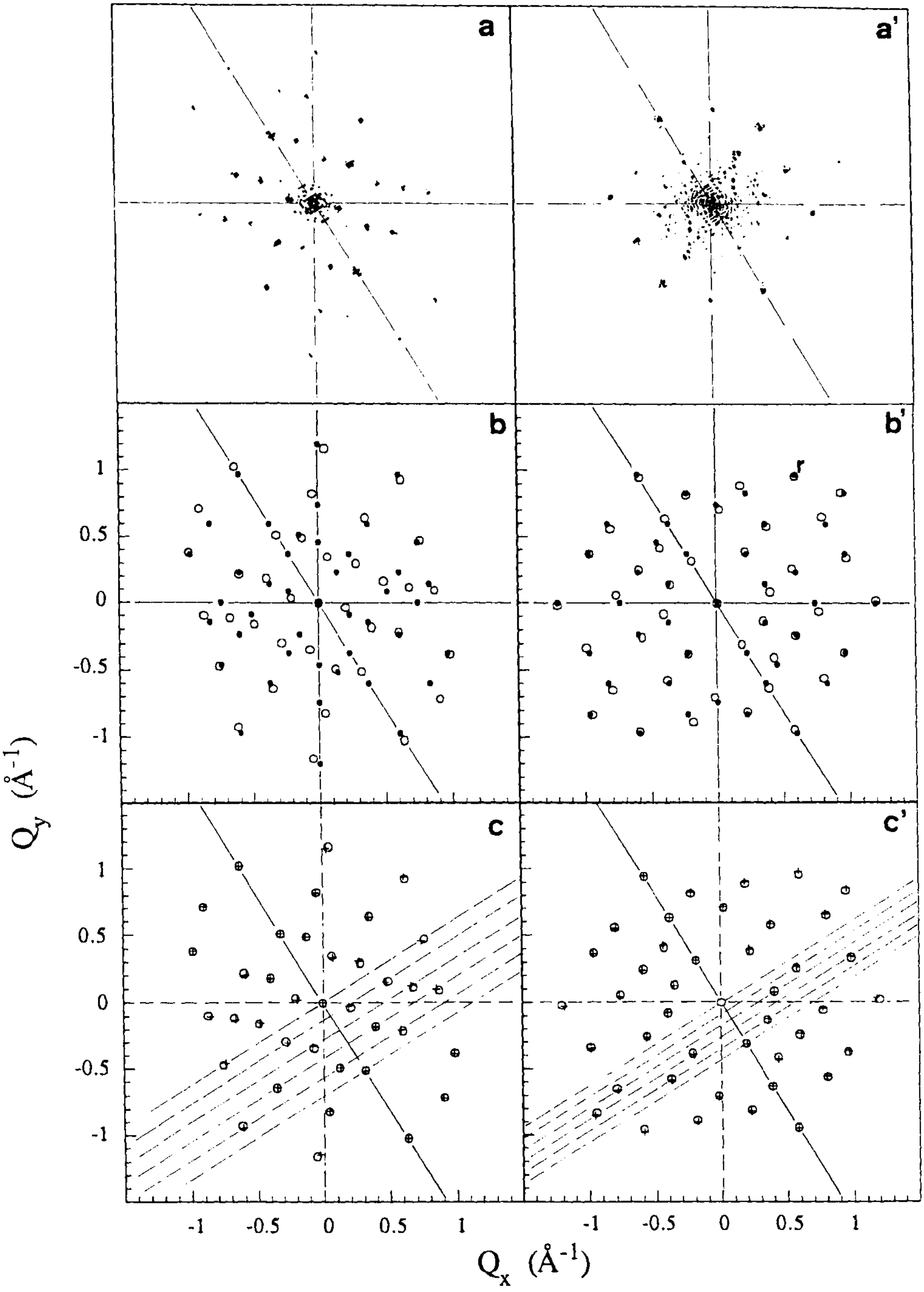

Structural analysis of the platelets of pentagonal structure: (*a*), (*a'*) the computer Fourier transforms of platelets of periods 10·45 and 16·9 Å respectively, where the directions of twofold and fivefold axes of the previous icosahedral state are indicated; (*b*), (*b'*) the reflection positions observed from the previous computer Fourier transforms (○) compared with those of the icosahedral state (●); (*c*), (*c'*) the reflection positions calculated from eqns (1) and (2) and matrices (3) and (4) (+) compared with those experimentally observed (○). The reflection labelled r, corresponding to 0/1 1/1 0/0, is at 1·139 $Å^{-1}$ (see table and Menguy *et al.* (1993a) for an indexing of the patterns). As explained in the text, all reflections can be situated on successive orders of (0000 *l*) Laue zones perpendicular to the fivefold axis of the pentagonal structures (sets of parallel lines); along these axes the indexing of the reflections are then (00005*n*) with $n \in Z$.

h/h'	k/k'	l/l'	Reflection symmetry	$\lvert G_{/\!/}\rvert$ (Å^{-1})	$\lvert G_{\perp}\rvert$ (Å^{-1})	$\Delta Q_{/\!/,x}$	$\Delta Q_{/\!/,y}$
			Pentagonal approximant of second order (10·45 Å)				
$\bar{1}/0$	$0/1$	$0/0$	12	0·704	0·704	−0·054	0·087
$0/\bar{1}$	$1/1$	$0/0$	12	1·139	0·435	0·033	−0·054
$\bar{2}/1$	$3/\bar{1}$	$0/0$	60	0·531	2·675	−0·020	0·021
$0/0$	$\bar{2}/2$	$0/0$	30	0·458	1·940	−0·069	0·112
$0/0$	$2/0$	$0/0$	30	0·740	1·198	0·043	−0·081
$0/0$	$0/2$	$0/0$	30	1·198	0·740	−0·050	0·036
$\bar{1}/1$	$1/0$	$0/0$	12	0·435	1·139	−0·053	0·074
$1/0$	$0/1$	$0/0$	12	0·704	0·704	0·019	−0·042
$0/1$	$1/1$	$0/0$	12	1·139	0·435	−0·020	0·041
$3/\bar{1}$	$\bar{3}/2$	$0/0$	60	0·519	3·337	0·024	−0·072
$2/0$	$\bar{2}/2$	$0/0$	60	0·870	2·279	−0·020	−0·012
$2/0$	$0/0$	$0/0$	30	0·740	1·198	0·064	−0·115
$\bar{1}/2$	$2/\bar{1}$	$0/0$	60	0·840	2·062	−0·043	0·047
$\bar{1}/1$	$3/2$	$0/0$	20	0·245	2·716	0·025	−0·052
$1/0$	$2/\bar{1}$	$0/0$	20	0·396	1·679	−0·024	0·039
$0/1$	$\bar{1}/1$	$0/0$	20	0·641	1·037	0·001	−0·013
$1/1$	$1/0$	$0/0$	20	1·037	0·641	−0·014	0·012
$\bar{1}/2$	$0/1$	$0/0$	60	1·022	1·390	−0·078	0·114
			Pentagonal approximant of third order (16·9 Å)				
$\bar{1}/1$	$1/0$	$0/0$	12	0·435	1·139	−0·036	0·059
$\bar{1}/0$	$0/1$	$0/0$	12	0·704	0·704	0·021	−0·034
$0/\bar{1}$	$1/1$	$0/0$	12	1·139	0·435	−0·016	0·025
$1/\bar{1}$	$\bar{1}/2$	$0/0$	60	0·859	1·653	−0·001	0·016
$0/0$	$2/0$	$0/0$	30	0·740	1·198	−0·021	0·036
$\bar{1}/1$	$\bar{1}/2$	$0/0$	60	0·859	1·653	0·040	−0·059
$\bar{1}/1$	$1/0$	$0/0$	12	0·435	1·139	0·009	−0·013
$1/0$	$0/1$	$0/0$	12	0·704	0·704	−0·011	0·024
$0/1$	$1/1$	$0/0$	12	1·139	0·435	0·002	0·013
$\bar{1}/2$	$0/1$	$0/0$	60	1·022	1·39	0·029	−0·051
$1/1$	$\bar{1}/2$	$0/0$	60	1·274	1·359	0·023	0·004
$0/1$	$\bar{1}/1$	$0/0$	20	0·641	1·037	0·027	−0·027
$1/1$	$1{\cdot}0$	$0/0$	20	1·037	0·641	−0·017	0·035
$0/2$	$0/0$	$0/0$	30	1·198	0·740	−0·002	−0·016
$1/0$	$2/\bar{1}$	$0/0$	20	0·396	1·679	−0·036	0·060
$2/0$	$0/0$	$0/0$	30	0·740	1·198	−0·028	0·060
$1/0$	$\bar{2}/1$	$0/0$	20	0·396	1·679	0·014	−0·009
$0/1$	$1/\bar{1}$	$0/0$	20	0·641	1·037	0·004	0·007
$1/1$	$\bar{1}/0$	$0/0$	20	1·037	0·641	0·009	0·002
$\bar{2}/2$	$2/\bar{2}$	$0/0$	60	0·647	2·741	0·022	−0·048
$\bar{1}/2$	$0/\bar{1}$	$0/0$	60	1·022	1·39	0·025	−0·038

Indexing of the icosahedral reflections shown in fig. 2 and from which the reflection shift coordinates $\Delta Q_{/\!/,x}$ and $\Delta Q_{/\!/,y}$ observed with the deformed icosahedral phase have been determined.

more horizontal and one more vertical row of coefficients. In order to determine these extra coefficients, we have first checked that the platelet structures exhibit one axis of fivefold symmetry parallel to the periodic reflection row from 36° rotations about this axis and computer Fourier transforms of the successively observed HREM images. From this investigation, we have found that the Fourier power spectra are always identical through alternate mirror symmetry operations and thus concluded that the platelet structures both have a fivefold axis of symmetry. It was then easy to define a system of equations from which all extra-coefficient values were found to be equal to zero. In three dimensions, the linear phason strain field matrices are finally

$$\varepsilon_{/\!/\perp}10{\cdot}45=\left(\frac{-1}{\tau^2}\right)^2\frac{1}{4^{1/2}}\begin{bmatrix}-1 & -\tau^{-1} & 0\\ \tau & 1 & 0\\ 0 & 0 & 0\end{bmatrix} \tag{5}$$

and

$$\varepsilon_{/\!/\perp}16{\cdot}9=\left(\frac{-1}{\tau^2}\right)^3\frac{1}{5^{1/2}}\begin{bmatrix}-1 & -\tau^{-1} & 0\\ \tau & 1 & 0\\ 0 & 0 & 0\end{bmatrix}. \tag{6}$$

From such matrices of shear in $E_\perp$, it can be verified that the 10·45 and 16·9 Å periods determined from both the reciprocal space (electron diffraction patterns) and the direct space (high-resolution electron micrographs), that is as related by the metric $dd^* = 2\pi$, are in good agreement with the displacement of icosahedral reflections in a 6D reciprocal space cut representation. For instance, figs. 3 (*a*)–(*c*) are sections of 6D reciprocal lattices spanned by two fivefold directions, each one into $E^*_{/\!/}$ (de Boissieu 1989). In the case of the undeformed hyperlattice (the icosahedral state) (fig. 3 (*a*)), the projected nodes of Z_6 on $E^*_{/\!/}$ are along a quasiperiodic sequence but, after applications of the $\varepsilon_{/\!/\perp 10\cdot45}$ and $\varepsilon_{/\!/\perp 16\cdot9}$ shear matrices (figs. 3 (*b*) and (*c*) respectively), their resulting displacements are such that the projected nodes on $E^*_{/\!/}$ appear to be along periodic sequences.

It is also easy to verify that such analyses are in agreement with the electron diffraction results. The two selected-area electron diffraction patterns shown in fig. 4

Fig. 3

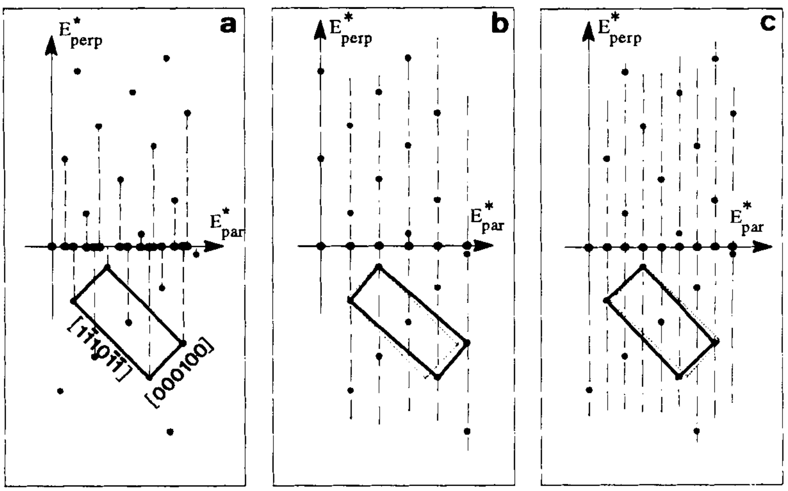

Visualization of the shear effects on a rational section of the Z_6^* reciprocal hyperspace spanned by two fivefold vectors belonging respectively to the subspaces $E^*_{/\!/}$ and $E^*_\perp$, where the section of the hypercubic is defined from the vectors [000100] and [$1\bar{1}10\bar{1}\bar{1}$]: (*a*) the icosahedral state where the projected nodes are along a quasiperiodic sequence; (*b*), (*c*) 10·45 and 16·9 Å pentagonal approximants respectively, where after application of the shear matrices the projected nodes are along periodic sequences.

are successively related firstly to the platelet structure of period 10·45 Å exhibiting several orientations of its fivefold symmetry axis along fivefold directions of the icosahedral point group and secondly to the 16·9 Å platelet structure. We have performed a simulation of the reflection positions observed on these experimental patterns by considering in both cases only the two variants of orientation where periodic rows of reflections are parallel to the two fivefold icosahedral axes contained in the diffraction plane. In fig. 4, the simulated patterns exhibit reflection positions which correspond exactly to those observed on the electron diffraction patterns.

§ 3. Theoretical estimate of the pentagonal shear matrices

The shear matrices can be easily determined by a procedure recently formulated by Gratias (1992).

In the R_6 hyperspace, the linear phason field $\boldsymbol{\varepsilon}^0$ shears in a parallel direction to $E_\perp$ the $\mathbf{r}^0_{/\!/\,\mathrm{ico}}$ and $\mathbf{r}^0_{\perp\mathrm{ico}}$ components in $E_{/\!/}$ and $E_\perp$ of a 6D vector $\mathbf{r}^0_6$ of the Z_6 lattice in such a way that the new components $\mathbf{r}^0_{/\!/}$ and $\mathbf{r}^0_\perp$ are given by the matrix product:

$$\begin{bmatrix} \mathbf{r}^0_{/\!/} \\ \mathbf{r}^0_\perp \end{bmatrix} = \begin{bmatrix} \mathbf{Id} & 0 \\ \boldsymbol{\varepsilon}^0 & \mathbf{Id} \end{bmatrix} \begin{bmatrix} \mathbf{r}^0_{/\!/\,\mathrm{ico}} \\ \mathbf{r}^0_{\perp\mathrm{ico}} \end{bmatrix}, \qquad (7)$$

where **Id** is the identity matrix.

Fig. 4

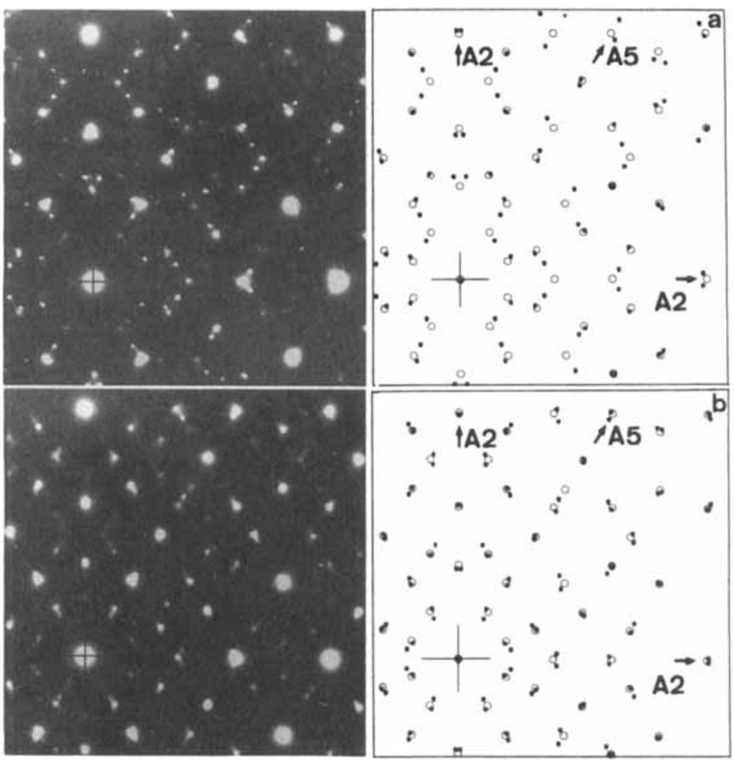

Comparison between electron diffraction and simulated patterns: (*a*) for the pentagonal approximant of period 10·45 Å, (*b*) for the pentagonal approximant of period 16·9 Å.

In the reciprocal R_6^* hyperspace, the $\mathbf{Q}^0_{/\!/\mathrm{ico}}$ and $\mathbf{Q}^0_{\perp\mathrm{ico}}$ components in $E^*_{/\!/}$ and $E^*_{\perp}$ of $\mathbf{Q}^0_6$ transform as

$$\begin{bmatrix}\mathbf{Q}^0_{/\!/}\\ \mathbf{Q}^0_{\perp}\end{bmatrix}=\begin{bmatrix}\mathbf{Id} & -{}^{\mathrm{tr}}\varepsilon^0\\ 0 & \mathbf{Id}\end{bmatrix}\begin{bmatrix}\mathbf{Q}^0_{/\!/\mathrm{ico}}\\ \mathbf{Q}^0_{\perp\,\mathrm{ico}}\end{bmatrix}. \tag{8}$$

The shear ε^0 of the hyperlattice leads to an approximate three-dimensional periodic structure if three vectors of Z_6 are brought into $E_{/\!/}$, that is if

$$\mathbf{r}^0_{\perp}=\mathbf{r}^0_{\perp\mathrm{ico}}+\varepsilon^0\mathbf{r}^0_{/\!/\mathrm{ico}}=0 \quad \text{or} \quad \varepsilon^0\mathbf{r}^0_{/\!/\mathrm{ico}}=-\mathbf{r}^0_{\perp\mathrm{ico}}. \tag{9}$$

Let $\mathbf{r}^0_{i\mathrm{ico}}$, $i=1$–3; these three basis vectors, with components $x^0_{i\mathrm{ico}}$, $y^0_{i\mathrm{ico}}$, $z^0_{i\mathrm{ico}}$ in an orthogonal reference spanned by twofold icosahedral axes. The shear matrix is then determined from the matrix product:

$$\varepsilon^0=-\begin{bmatrix}x^0_{1\perp\mathrm{ico}} & x^0_{2\perp\mathrm{ico}} & x^0_{3\perp\mathrm{ico}}\\ y^0_{1\perp\mathrm{ico}} & y^0_{2\perp\mathrm{ico}} & y^0_{3\perp\mathrm{ico}}\\ z^0_{1\perp\mathrm{ico}} & z^0_{2\perp\mathrm{ico}} & z^0_{3\perp\mathrm{ico}}\end{bmatrix}\begin{bmatrix}x^0_{1\,/\!/\mathrm{ico}} & x^0_{2\,/\!/\mathrm{ico}} & x^0_{3\,/\!/\mathrm{ico}}\\ y^0_{1\,/\!/\mathrm{ico}} & y^0_{2\,/\!/\mathrm{ico}} & y^0_{3\,/\!/\mathrm{ico}}\\ z^0_{1\,/\!/\mathrm{ico}} & z^0_{2\,/\!/\mathrm{ico}} & z^0_{3\,/\!/\mathrm{ico}}\end{bmatrix}^{-1}. \tag{10}$$

The choice of the $\mathbf{r}^0_i$ vectors define ε^0 but also the order of the approximant phase and its point-group symmetry. The approximant order is defined as for the rational approximate of the golden mean τ, that is the ratio p/q of two successive terms of the Fibonnaci series: zeroth order for $p/q=1/0$, first order for $p/q=1/1$, second order for $p/q=2/1$, etc. Since for successive approximate orders of a same structure symmetry, the vectors brought into $E_{/\!/}$ are τ inflated ($\mathbf{r}^{n+1}_{/\!/\mathrm{ico}}=\tau\mathbf{r}^{n}_{/\!/\mathrm{ico}}$), the shear matrix corresponding to an approximant structure of nth order is defined as

$$\varepsilon^n=\left(\frac{-1}{\tau^2}\right)^n\varepsilon^0. \tag{11}$$

The cell parameters of the approximant structure are related to the $a_{6\mathrm{D}}$ hypercubic cell parameter. For instance, the Al–Fe–Cu rhombohedral structure of cell parameters $a_{\mathrm{R}}=32{\cdot}16$ Å and $\alpha=36°$, corresponds to three twofold icosahedral vectors τ^3 inflated (e.g. 101000, 011000 and 110000) brought into $E_{/\!/}$ and whose modulus is equal to $\tau^4 a_{6\mathrm{D}}\,2^{1/2}/(\tau+2)^{1/2}=32{\cdot}16$ Å. It is straightforward to deduce that there are two types of shear matrix to be considered depending on the type of threefold icosahedral axis (either $[\tau\tau\tau]$ or $[\tau^2 10]$) which becomes after shearing parallel to the threefold axis of the rhombohedral structure:

$$\varepsilon^3_{\mathrm{i}\to\mathrm{rh}(\tau\tau\tau)}=\left(\frac{-1}{\tau^2}\right)^3\frac{1}{2}\begin{bmatrix}\tau-2 & 2\tau-1 & \tau-3\\ \tau-3 & \tau-2 & 2\tau-1\\ 2\tau-1 & \tau-3 & \tau-2\end{bmatrix} \tag{12}$$

and

$$\varepsilon^3_{\mathrm{i}\to\mathrm{rh}(\tau^2 10)}=\left(\frac{-1}{\tau^2}\right)^3\begin{bmatrix}\tau-1 & \tau-3 & 0\\ 0 & \tau-1 & 0\\ 0 & 0 & -\tau\end{bmatrix}. \tag{13}$$

Note that the shear expression given in eqn. (12) is exactly equivalent to that proposed by Ishii (1989, 1990) as a sum of two shears where the icosahedral-to-rhombohedral transformation is assumed to be the result of a two-step deformation, cubic and pentagonal. For this, Ishii's arguments are based on considerations on the irreducible representations of the icosahedral point group related to phason displacements.

In order to interpret our experimental results, Gratias' formalism has now to be applied in order to generate a pentagonal structure. This application is, however, more complex than in the case of a 3D periodic approximant crystal because the exact structural characteristics of the pentagonal phases (e.g. their super space group) are unknown. The pentagonal symmetry is generated by bringing a single fivefold 6D basis vector into $E_{/\!/}$ of a sum of vectors which conserves the fivefold symmetry. In the following, two cases of shear are examined.

(1) A fivefold basis vector $\mathbf{r}_1^0$ is brought into $E_{/\!/}$. The $\boldsymbol{\varepsilon}^0$ matrix is determined after noting that all 6D vectors whose components in $E_{/\!/}$ are perpendicular to $\mathbf{r}_1{}^0{}_{/\!/}$ must have their components unchanged in $E_\perp$. If two of them are $\mathbf{r}_2^0$ and $\mathbf{r}_3^0$, then from eqn. (8),

$$\boldsymbol{\varepsilon}^0_{i\to p} = -\begin{bmatrix} x^0_{1\perp ico} & 0 & 0 \\ y^0_{1\perp ico} & 0 & 0 \\ z^0_{1\perp ico} & 0 & 0 \end{bmatrix} \begin{bmatrix} x^0_{1\,/\!/ico} & x^0_{2\,/\!/ico} & x^0_{3\,/\!/ico} \\ y^0_{1\,/\!/ico} & y^0_{2\,/\!/ico} & y^0_{3\,/\!/ico} \\ z^0_{1\,/\!/ico} & z^0_{2\,/\!/ico} & z^0_{3\,/\!/ico} \end{bmatrix}^{-1} . \tag{14}$$

For the zeroth order of a pentagonal approximant structure with $\mathbf{r}_1^0 = (000100)$, that is $\mathbf{r}^0_{1\,/\!/} = (\bar{1}\tau 0)$, one obtains

$$\boldsymbol{\varepsilon}^0_{i\to p} = \frac{1}{5^{1/2}} \begin{bmatrix} 1 & -\tau & 0 \\ \tau^{-1} & -1 & 0 \\ 0 & 0 & 0 \end{bmatrix} . \tag{15}$$

In the reciprocal space, the transposed matrix with a minus sign ($-{}^{tr}\boldsymbol{\varepsilon}^0_{ico\to p}$) has to be considered. The experimental matrices, as given by eqns. (5) and (6), are found again if $-{}^{tr}\boldsymbol{\varepsilon}^0_{ico\to p}$ is multiplied by the factors $-(-1/\tau^2)^2$ and $-(-1/\tau^2)^3$. Although the sign of these factors is not correct, the pentagonal approximates would then be of second and third order. However, in that case, the measured periods of 10·45 and 16·9 Å for these pentagonal phases should correspond to $\tau^2|\mathbf{r}^0_{1\,/\!/}|/l$ and $\tau^3|\mathbf{r}^0_{1\,/\!/}|/l$ respectively, where $|\mathbf{r}^0_{1\,/\!/}| = a_{6D}/2^{1/2}$ and l is an integer directly related to the Miller's indexing of the first reflection $000 0l$ observed along the pentagonal axis. As both measured periods are very close to the factors

$$\frac{a_{6D}}{2^{1/2}} \frac{2}{5^{1/2}} \tau^2 = 10{\cdot}447\ \text{Å}$$

and

$$\frac{a_{6D}}{2^{1/2}} \frac{2}{5^{1/2}} \tau^3 = 16{\cdot}905\ \text{Å},$$

this means that the fivefold basis vector should have a modulus of the form

$$|r^n{}_{/\!/}| = \frac{a_{6D}}{2^{1/2}}\, 2 \times 5^{1/2} \tau^n . \tag{16}$$

Therefore a τ^n-inflated fivefold basis vector of the previous type does not explain our experimental results.

(2) From eqn. (16) it appears that, depending on the l value, there are *a priori* several solutions for selecting a convenient fivefold basis vector. However, the value of l must be consistent with the extinction rules of pentagonal space group as well as with the HREM images. With this restrictive condition, there is one solution which consists to bring into $E_{/\!/}$ a fivefold τ^n- inflated vector $\mathbf{r}_1^n$ whose components in $E_{/\!/}$ are $\tau^n(2-4\tau, 4+2\tau, 0)$. This corresponds for the order $n=0$ to a fivefold $\mathbf{r}_1^0$ vector of the type $(2\bar{2}20\bar{2}\bar{2})$ which is the sum of either fivefold basis vectors, namely

$$(2\bar{2}20\bar{2}\bar{2}) = [(100000) + (0\bar{1}0000) + (001000) + (0000\bar{1}0) + 00000\bar{1})],$$

or of twofold vectors, namely

$$(2\bar{2}20\bar{2}\bar{2}) = (1\bar{1}0000) + (0\bar{1}1000) + (0010\bar{1}0) + (0000\bar{1}1) + (10000\bar{1}).$$

In that case, the matrix (15) is obtained but with the reverse sign, in agreement with the experimental matrices (5) and (6) for the orders $n=2$ and $n=3$ (the corresponding fivefold vectors are $\mathbf{r}_1^2=(3\bar{3}35\bar{3}\bar{3})$ and $\mathbf{r}_1^3=(4\bar{4}4\,10\,\bar{4}4)$). As $|\mathbf{r}^n_{/\!/}|$ is of the form

$$|\mathbf{r}^n_{/\!/}| = \frac{a_{6\mathrm{D}}}{2^{1/2}} 2 \times 5^{1/2}\tau^n,$$

from eqn. (16) an l value equal to 5 is justified.

In figs. 2 (c) and (c'), it is shown that the reflections of the pentagonal approximants are located in planes periodically spaced along the fivefold symmetry axis. These planes can then be considered as corresponding to successive orders of (0000l) Laue zones. As the first reflection observed along the fivefold symmetry axes is situated, in both cases, on the fifth plane, it can be deduced that the simplest indexing to attribute to this reflection is (00005) and (00005n), with $n \in Z$ for higher-order reflections. This implies periodic parameters for the pentagonal phases equals to $5 \times 10{\cdot}45$ Å $= 52{\cdot}25$ Å and $5 \times 16{\cdot}905$ Å $= 84{\cdot}525$ Å, as indicated in the high-resolution micrograph in fig. 1. Such periodicities seem to be effectively confirmed if we note that in this micrograph, and also in the micrograph in fig. 5 for a large platelet of the pentagonal approximant of second order, that repetitions of the white dots along the fivefold symmetry axis occur at these distances.

§4. Discussion

The present results can be interpreted using the ideas which we have proposed to explain the modulated state of the icosahedral phase (Menguy *et al.* 1992b, 1993c). The modulated state of the icosahedral phase (Menguy *et al.* 1992b, 1993c). The modulated state which has been assigned to sine phason waves propagating along fivefold axes can be considered as the precursor state, similarly to an ordering spinodal. As the amplitude of the sine phason wave increases with time, it can lock on to an alternate structure of domains of the two pentagonal phases coherently bounded at their interfaces. In each case, the shear remains parallel to fivefold axes in $E_\perp$ and is along the same fivefold axes in $E_{/\!/}$. The alternate 'slopes' of two approximants (ε^n and ε^m for n even and m odd), while keeping the global phason strain equal to zero, produces two different domain sizes. Therefore satellites of higher order should appear near the

Fig. 5

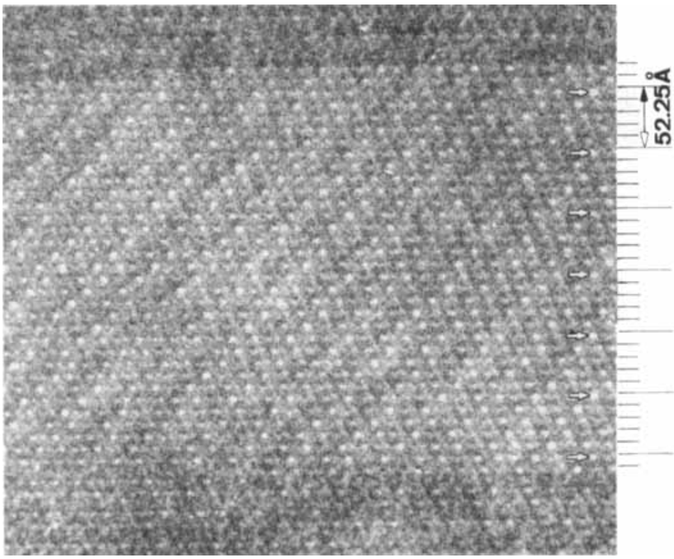

High-resolution electron micrograph of the pentagonal approximant of second order: the periodicity of white dots observed along the fivefold axis justifies the cell parameter $c = 52{\cdot}25$ Å. Note that such a thick platelet results in the evolution of a mixed state of two pentagonal structures as a function of time for an annealing treatment at 600°C.

icosahedral reflections when the sine wave reaches the locking point. This has indeed been observed and is under study (Menguy, Audier, Guyot and Vacher 1993b)†.

In further work, we shall examine how this state of pentagonal approximants transforms into the crystalline multidomain structure of the rhombohedral phase. From first investigations, we have verified that the pentagonal phases do finally transform into the rhombohedral phase but after a very long annealing treatment (about 30 days at 600°C). However, this step of transformation is not direct; we have found that, as a function of the annealing time at 600°C, the average thickness and spacing between platelets of the second-order pentagonal approximant increase. The third-order pentagonal approximant curiously transforms into a new 3D quasiperiodic structure which is not icosahedral, however.

Finally let us note that, in a recent article, Bancel (1993) has reported identification of a Al–Fe–Cu pentagonal structure of period 52·31 Å. His result is in agreement with ours.

† However, as the basis fivefold vectors of the pentagonal phases are close to the fivefold directions $\langle 01111\bar{1}\rangle$, the wave-vectors related to a modulated icosahedral structure should also be along these directions instead of $\langle 100000\rangle$, as has been assumed previously. Note that such a change does not modify the modulus of the polarization vectors which have been determined from the analysis of the X-ray diffraction data, because the vectors $[100000]$ and $[01111\bar{1}]$ are symmetric with respect to the $E_{\parallel}$ subspace and their projection ratios into $E_{\parallel}$ are the same $(2^{1/2})$.

References

AUDIER, M., and GUYOT, P., 1989, *Quasicrystals and Incommensurate Structures In Condensed Matter, Proceedings of the Third International Meeting on Quasicrystals*, Vista Hermosa, Mexico, 1989, edited by M. J. Yacaman, D. Romeu, V. Castano and A. Gomez (Singapore: World Scientific), p. 288; 1990, *Proceedings of the Anniversary Adriatic Research Conference on Quasicrystals*, Trieste, edited by M. V. Jaric and S. Lundqvist (Singapore: World Scientific), p. 74.

AUDIER, M., GUYOT, P., and BRÉCHET, Y., 1990, *Phil. Mag. Lett.*, **61,** 55.

BANCEL, P., 1989, *Phys. Rev. Lett.*, **63,** 2741; 1991, *Quasicrystals: the State of the Art*, edited by D. P. Divicenzo and P. Steinhardt (Singapore: World Scientific), p. 17; 1993, *Phil. Mag. Lett.*, **67,** 43.

CAHN, J. W., SHECHTMAN, D., and GRATIAS, D., 1986, *J. Mater. Res.*, **1,** 13.

CALVAYRAC, Y., QUIVY, A., BESSIÈRE, M., LEFEBVRE, S., CORNIER-QUIQUANDON, M., and GRATIAS, D., 1990, *J. Phys., Paris*, **51,** 417.

DE BOISSIEU, M., 1989, Thesis, Institute National Polytechnique de Lorraine.

GRATIAS, D., 1992, *Rational Approximants Obtained from Shear into $E_\perp$, Groupement de Recherches 5 Meeting*, Gif sur Yvette, 1992.

ISHII, Y., 1989, *Phys. Rev.* B, **39,** 11862; 1990, *Phil. Mag. Lett.*, **62,** 393; 1992, *Phys. Rev.* B, **45,** 5228.

JANSSEN, T., 1991, *Europhys. Lett.*, **14,** 131.

JARIC, M., and NELSON, R., 1988, *Phys. Rev.* B, **59,** 4458.

LUBENSKY, T. C., SOCOLAR, J. E. S., STEINHARDT, P. J., BANCEL, P. A., and HEINEY, P., 1986, *Phys. Rev. Lett.*, **57,** 1440.

MENGUY, N., AUDIER, M., DE BOISSIEU, M., GUYOT, P., BOUDARD, M., and JANOT, C., 1993a, *Phil. Mag. Lett.*, **67,** 35.

MENGUY, N., AUDIER, M., and GUYOT, P., 1992a, *Phil. Mag. Lett.*, **65,** 7.

MENGUY, N., AUDIER, M., GUYOT, P., and VACHER, M., 1993b (to be published).

MENGUY, N., DE BOISSIEU, M., GUYOT, P., AUDIER, M., ELKAIM, E., and LAURIAT, P., 1992b, *J. non-crystalline Solids;* 1993c, *J. Phys., Paris* (in press).

QIU, S. Y., and JARIC, M. V., 1989, *Proceedings of the Anniversary Adriatic Research Conference on Quasicrystals*, Trieste, 1989, edited by M. V. Jaric and S. Lundqvist (Singapore: World Scientific), p. 19.

SIMON, J. P., LYON, O., and DE FONTAINE, D., 1985, *J. appl. Crystallogr.*, **18,** 30.